ISSN (Print) 1226-1750
ISSN (Online) 2233-6656
Journal of Magnetics 29(2), 172-178 (2024) https://doi.org/10.4283/JMAG.2024.29.2.172

Efficiency Application of Monte Carlo Simulation and HPGe Detector Using Mapping Method

Eun-Sung Jang[1]* and Bo-Seok Chang[2]*

[1]Department of Radiation Oncology, Gospel Hospital, Kosin University, Busan 49267, Republic of Korea
[2]Depart of Radiological Science, Kaya University, Gimhae 50830, Republic of Korea

(Received 26 February 2024, Received in final form 26 April 2024, Accepted 20 May 2024)

In order to obtain the detection efficiency according to the distance around the detector, the total energy peak efficiency was used, and the grid mapping method was used to investigate axis-symmetry. The detector was measured at 0.5 cm intervals up to 5 cm in the x, z, direction, and 5.5 cm in the y direction. The efficiency of the cylinder beaker and marinelli beakers at the center of the ^{134}Cs 604 keV detector was compared with the efficiency of the mapping method. For cylinder beakers, the efficiency was 0.0412 ± 0.002, and the efficiency by mapping was 0.040 ± 0.001, which was consistent within 3 % of the uncertainty range. For Marinelli beakers, the efficiency was 0.0242 ± 0.002 mapping efficiency was 0.0248 ± 0.0013. It was confirmed that precise measurement of radioactive sources with volume was possible when measured at each point around the detector.

Keywords : mapping, monte carlo simulation, Computed Tomography (CT), HPGe detector, electromagnetic X-ray image

1. Introduction

The problem of HPGe detector efficiency has been studied a lot because of the unique characteristics and detection methods of each detector in γ-ray spectroscopy [1-8]. The detector efficiency is affected by the same location from the detector to the source, the same geometry between the unknown source and the CRM source, and the same energy. The mapping method was used to investigate the detection efficiency according to the distance around the detector and the axis-symmetry of the detector determination. The total energy peak efficiency was measured by changing the position of the γ-ray dotted line source at 5 mm intervals on the three sides around the HPGe coaxial detector using a lattice mapping method. Efficiency symmetry of the detector was observed by measuring at 5 mm intervals in I using ^{133}Ba, ^{134}Cs, and ^{152}Eu sources. After scanning the detector at 5mm slice intervals in computed tomography, the efficiency values measured in the obtained image and the results compared with the calculations by computer simulation (PENELOPE, GEANT4) were applied to the mapping method. In this study, measurements and calculations were compared and analyzed for the total energy peak efficiency while changing the position of the dotted source in the axis and radial direction of the HPGe cylindrical detector using a grid mapping method in the self-made Moving Stage.In addition, we want to find out the efficiency and scope of the detector by measuring the efficiency of the images acquired from computed tomography and computer simulation.

2. Materials Method

2.1. The Monte carlo simulation for the mapping method improved by the CT

The only way to know inside of the detector is to use the data sheet from the manufacturer. The validation of the data sheet can be done by the CT Electromagnetic X-ray image. The center line of the detector was aligned to the center line of laser ray of CT (GE Lightspeed VCT 64) to take the picture inside of the detector with 120 keV, 130 mA in 5 mm slice from the end cap window to the mount cap base (Fig. 1).

The data collected by the CT and the manufacturer's data sheet were applied to the simulation (Fig. 2). The

*Corresponding author: Tel: +82-55-344-5231
Fax: +82-55-344-5284, e-mail: john430@naver.com

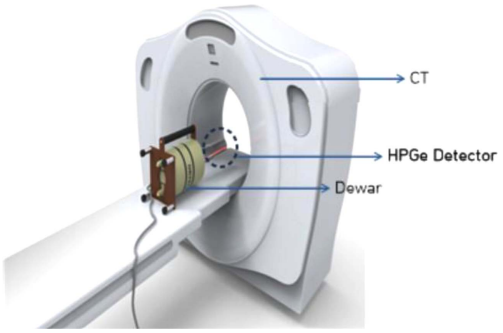

Fig. 1. (Color online) The center line of the detector was set up in line with the center line of the laser beam of CT.

detector structure was applied to the PENELOPE [9] and GEANT4 [10] code in the Monte Carlo simulation [9, 10]. The calculated efficiencies of the detector were used for both the mapping method and the study of the efficiency variation depending on the position and energy [9, 10].

2.2. The calibration of the HPGe detector using the CRM

The energy and efficiencies of the HPGe detector at each point were calibrated by the CRM. The geometric arrangement of the detector and the point source was measured at a distance of 0.5 cm from the surface of the detector Ge crystal sensitive layer. The CRM sources were the ^{133}Ba (53, 81, 160, 276, 302, 356, 383 keV), ^{134}Cs (604, 795 keV), and ^{1152}Eu (121, 244, 344, 411, 443, 778, 964, 1112, 1212, 1299, 1408 keV) point sources. They were used for getting the efficiencies from the low energy 53 keV to the high energy 1408 keV. The the number of the net counts was calculated by the fitting method.

which was used in the Gamma Vision. These net counts at each energy gave the efficiencies at different energies and fitted by the polynomial log function.

This fitted efficiencies at the different energies which given by the CRM were used for the mapping method.

$$\varepsilon(E) = \frac{NCi}{TAp} \tag{1}$$

where N is the number of net counts in the peak, T is ts the measuring time, A is the radionuclide activity, p is the photon emission probability [10] and Ci are corrections factors due to dead time, radionuclide decay and coincidence summing corrections.

2.3. The Efficiency variation depending on the energy and position

The efficiencies depend on the positions and energies. The position was varied by 0.5 cm intervals vertically and horizontally. The energies of ^{133}Ba (53, 81, 160, 276, 302, 356, 383 keV), ^{134}Cs (604, 795 keV), ^{152}Eu (121, 244, 344, 411, 443, 778, 964, 1112, 1212, 1299, 1408 keV) were measured and calculated. This efficiency ratio was calculated to check the validity of the simulation.

2.4. Efficiency ratio

The efficiency ratio was dened as the ratio of the calculated efficiency by using the simulation and the measured eciency in Eq. (2), (3). The uncertainty of the efficiency ratio was given by the uncertainty propagation [10].

The efficiency of the perfect Monte Carlo simulation should be exactly same with the measured efficiency. The Efficiency ratio can be one in the perfect simulation. The calculated efficiency was higher than the measured one because of the dead layer.

$$\text{Ratio(Y)} = \frac{\text{Calculate efficiency (a)}}{\text{Measure efficiency (b)}} \tag{2}$$

$$\sigma r = r\sqrt{\frac{\sigma a2}{a2} + \frac{\sigma b2}{b2}} \tag{3}$$

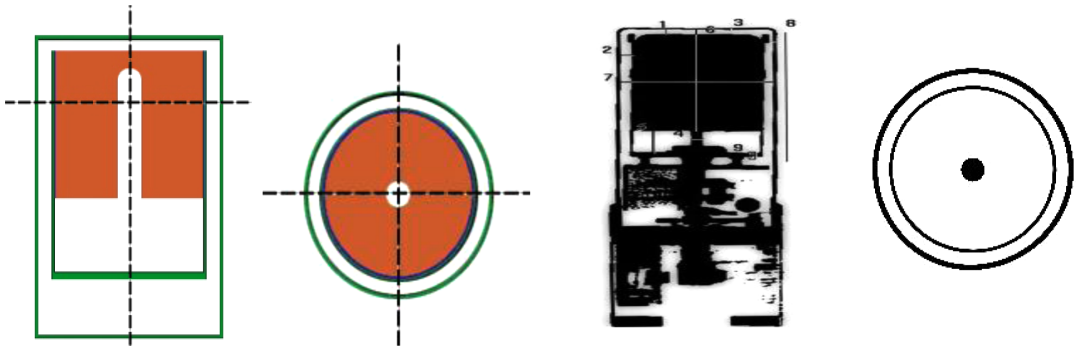

Fig. 2. (Color online) Schematic representation of the detector model (2D) used in the Monte Carlo calculations. CT Scanner taken of the Electromagnetic X-ray image HPGe detector to verify the geometric structure.

2.5. Efficiency measurement by separating the area I, II, and III

These efficiencies with the varying energies were obtained at the one point. The next 0.5 cm distance point was calibrated vertically and horizontally. The area I was the first section from the top of the endcap to the 5 cm above vertically and from the center of the detector to the end of the endcap horizontally. The area II was second section beside of the area I 5 cm vertically and 5.5 cm horizontally. The area III was the below of the area II 5 cm vertically and 5.5 cm horizontally. The Fig. 3 was shown this areas.

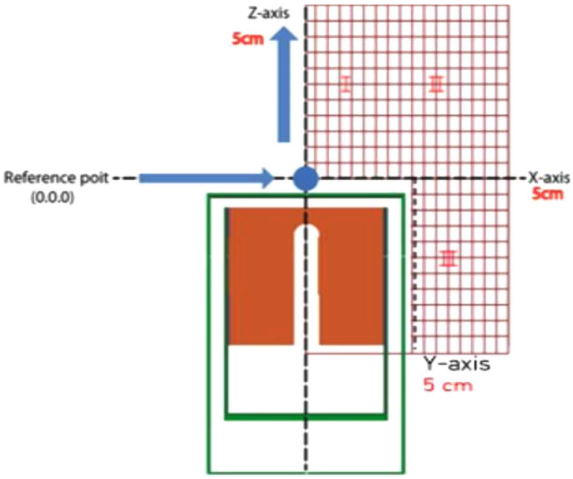

Fig. 3. (Color online) The source-detector geometry. Mapping method based on measurement points of the axis of symmetry (Z-axis) and radial direction (X-axis) and axial direction (Y-axis) of the point ray source at a designated location around the detector.

2.6. The mapping method

The above efficiencies can be used for the mapping method. The unknown radioactive source of the cylinder and Marinelli beaker can be measured by using the efficiency of the mapping method. The radius and height of cylinder radioactive source were all 3 cm. The mean value can be taken by adding efficiency from the origin (0,0,0) to 3 cm horizontally and 3 cm vertically and multiplied by 2. The mapping method was assuming the axial symmetry along the central line. The efficiency of the mapping method having the cylindrical geometry was averaged by the 16 efficiency values in this area. The Marinelli beaker had the geometry of the radius, 11 cm and height, 10 cm. The 161 efficiency values were used for this geometry. The uncertainty of this mapping method efficiency was calculated by the principle of the uncertainty propagation in the Eq. (4), (5).

$$\varepsilon ext \frac{\varepsilon 1 + \varepsilon 2 + \cdots + \varepsilon 16}{16} \tag{4}$$

$$\sigma \varepsilon ext \frac{1}{16} \sqrt{(\sigma 1)2 + (\sigma 2)2 + \cdots (\sigma 16)2} \tag{5}$$

3 Results

3.1. The calibration of the HPGe detector using the CRM

After energy calibration, the error in measurements and calculations from the low-energy region of 53 keV to the high-energy region of 1408 keV of the dotted line ^{133}Ba, ^{134}Cs and ^{152}Eu at a distance of 0.5 cm from the surface of

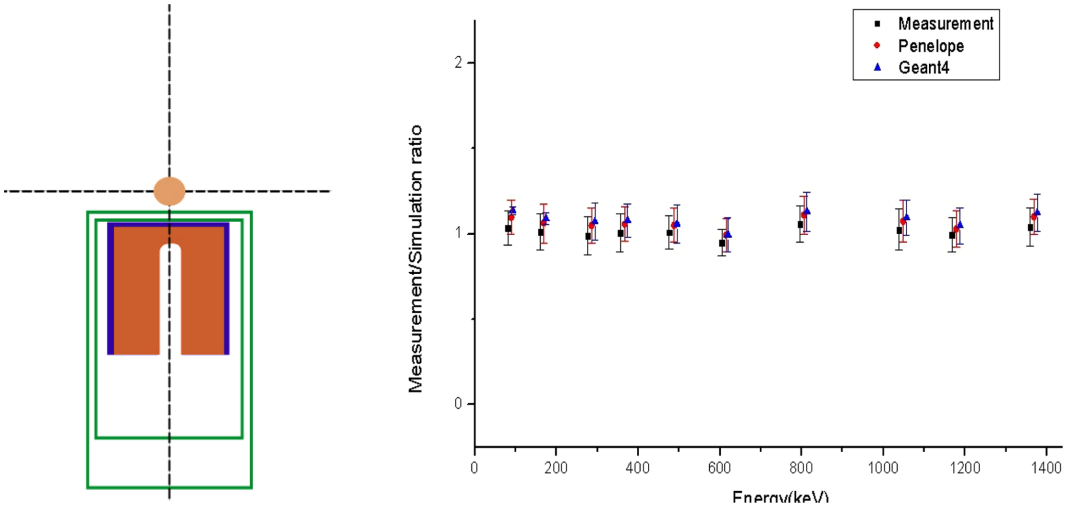

Fig. 4. (Color online) Compare the central axis dependence of the ratio of efficiency to low energy area ^{133}Ba (53, 81, 160, 276, 302, 356, 383 keV), ^{134}Cs (604, 795 keV), and high energy area ^{152}Eu (121, 244, 344, 344, 411, 443, 778, 964, 1112, 1299, 1408 keV) at a distance of 0.5 cm from the detector crystal plane.

the detector Ge crystal sensitive layer was well within 2.5 % (Fig. 4).

3.2. The Efficiency variation depending on the energy and position

The simulation was validated by the comparison of the efficiency ratio by the energies and distance. The measured and calculated value by the energies using point source ^{133}Ba, ^{134}Cs, ^{152}Eu on detector is shown in Fig. 5 The points sources was located 0.5 cm offset above the endcap. The efficiency ratio was shown in Fig. 5 versus Energies. The peak efficiency decreases as the energy increases because the proportion of gamma rays attenuated in the detector window consisting of Al endcap, Ge insensitive layer, etc. increases before reaching the detector sensitive layer. At peak efficiencies of ^{133}Ba, ^{134}Cs and ^{152}Eu, the uncertainty of measurements and calculations was well within 3 %.

3.3. Efficiency measurement by separating the area I, II, and III

Figs. 6, 7, 8 shows efficiencies by the position from the detector area I, II, III. The efficiency ratio of the area I was shown in the Fig. 6. The efficiencies depending on the distance was shown on the left of the Fig. 6. The efficiency ratio of the area II and III was shown in the Fig. 7 and Fig. 8, respectively. As in Figs. 6, 7, and 8, As shown in Figs. 6, 7, and 8, respectively, the results of measurement and computer simulation (PENELOPE, GEANT4) were well matched within the range of 3 % uncertainty [11, 12].

Figure 6 shows that when the distance is short, the efficiency of the dotted source located on the detector axis is inversely proportional to the distance from the detector, and the peak efficiency with the distance between the source and the detector decreases with increasing distance or with increasing energy. Furthermore, as the source approaches the detector, the total energy peak

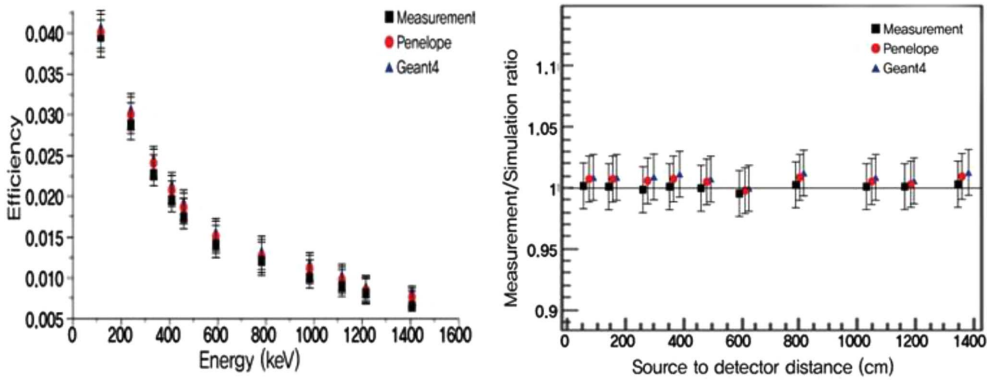

Fig. 5. (Color online) The measurement of the efficiency of the point source located in the center of the front of the detector and the calculated value can be seen in Fig. 5. If the distance is short, the efficiency of the dotted source located on the detector axis is inversely proportional to the distance from the detector, indicating that the peak efficiency according to the distance between the source and the detector decreases with increasing distance or with increasing energy.

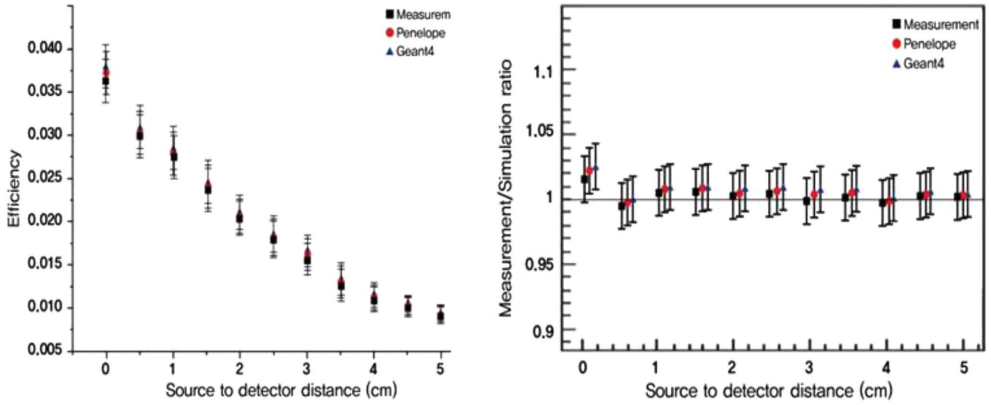

Fig. 6. (Color online) Simulated efficiency comparison with measured efficiency at an energy of 604 keV according to the distance between the detector and the source.

efficiency is reduced by the corner effect, which increases the proportion of gamma rays traveling to the corner with shorter path lengths in the sensitive region [13, 14]. From these results, it can be seen that the total energy peak efficiency of the HPGe detector shown as efficiency depends very sensitively on the distance between the source and the detector.

Figs. 6, 7, 8 shows efficiencies by the position from the detector area I, II, III. The efficiency ratio of the area I was shown in the Fig. 6. The efficiencies depending on the distance was shown on the left of the Fig. 6. The efficiency ratio of the area II and III was shown in the Fig. 7 and Fig. 8, respectively. As in Figs. 6, 7, and 8, As shown in Figs. 6, 7, and 8, respectively, the results of measurement and computer simulation (PENELOPE, GEANT4) were well matched within the range of 3 % uncertainty [11, 12].

Figure 6 shows that when the distance is short, the efficiency of the dotted source located on the detector axis is inversely proportional to the distance from the detector, and the peak efficiency with the distance between the source and the detector decreases with increasing distance or with increasing energy. Furthermore, as the source approaches the detector, the total energy peak efficiency is reduced by the corner effect, which increases the proportion of gamma rays traveling to the corner with shorter path lengths in the sensitive region [13, 14]. From these results, it can be seen that the total energy peak efficiency of the HPGe detector shown as efficiency depends very sensitively on the distance between the source and the detector.

Figures 7, 8 shows that the peak efficiency for low-energy gamma rays decreases with smaller distances in peak efficiency according to the axial and radial directions between the source and the detector due to the attenuation effect of increasing the proportion of gamma rays attenuated by increased path length in the detector window. It was confirmed that as the source approached

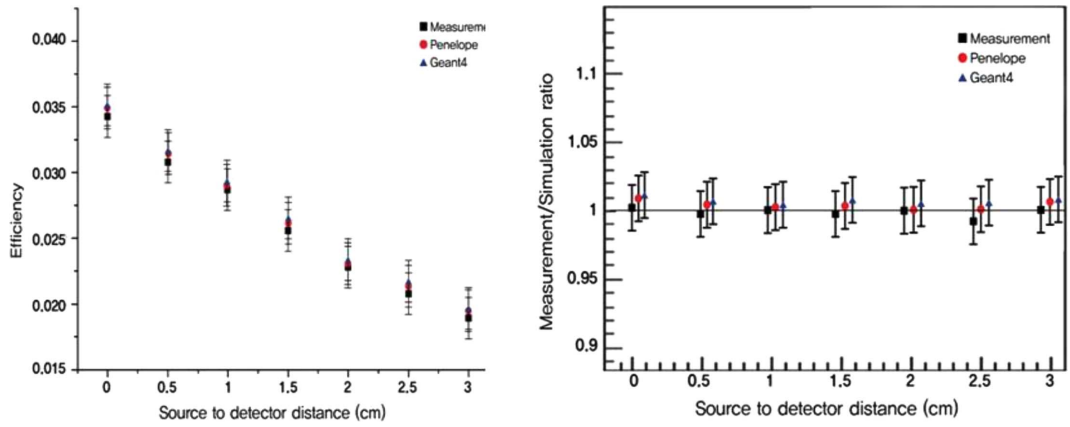

Fig. 7. (Color online) Comparison of simulated efficiency values with measured values of 604 keV energy efficiency according to distance movement of the detector and ^{134}Cs source in the vertical direction.

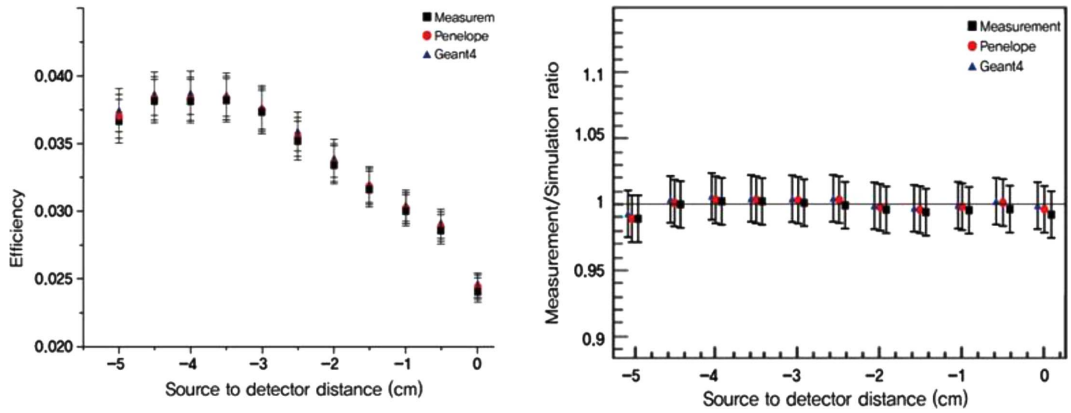

Fig. 8. (Color online) Comparison of simulated efficiency values with measured values of 604 keV energy efficiency according to distance movement of the detector and ^{134}Cs source in the horizontal direction.

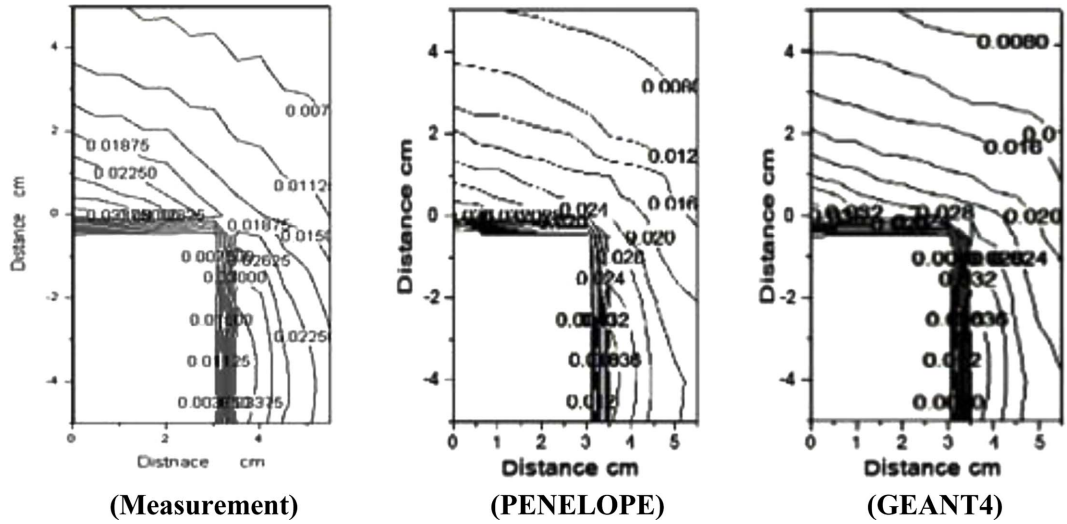

Fig. 9. Mapping by comparing measured values according to the distance between the detector and the source with efficiency values for the entire simulated area.

the detector, the peak efficiency decreased due to the edge effect, which increased the proportion of gamma rays traveling from the sensitive area to the corner with a shorter path length.

3.4. The mapping method

The equal efficiency line was shown in the Fig. 9 having the 0.004 intervals. The maximum efficiency was 0.036 ± 0.0029 over the area I, while the minimum one was 0.005 ± 0.00072 under the area III. These can be extended to the arbitrary geometry of the radioactive source. The mapping method efficiency of the HPGe detector for the cylinder and Marinelli beaker geometry was shown the below. The efficiency of the HPGe detector was measured by using the cylindrical CRM and Marinelli one. These efficiencies were compared with the efficiencies of the mapping method to validate of this method. The efficiency using the cylindrical CRM was 0.0412 ± 0.002, while the one of mapping method was 0.040 ± 0.001. The efficiency using the Marinelli geometry one was 0.0242 ± 0.002, and the mapping method efficiency was 0.0248 ± 0.0013. The uncertainty was calculated by the propagation of the uncertainty principle. The mapping method was validated by the experimental values with in the uncertainty range. The mapping method can be conducted by the experiment and the Monte Carlo simulation of the mapping method extend the usage of the mapping method. The measured efficiencies of the detector can be extended to the area which is not measured by the experiment. The map of the efficiencies by the experiment and the map of the efficiencies by the Monte Carlo simulation were matched within the uncertainty range. The efficiencies of the unmeasured area can be calculated by the Monte Carlo simulation and these can be used for the arbitrary geometry which is not covered by the experimental mapping method area (Fig. 9).

4. Conclusion

The efficiencies of the HPGe detector was depend on the geometry of the source and position and the energies [15-17]. The measurement can be done after calibration with the same geometry CRM sources [18, 19]. These arbitrary CRM are not available in any conditions. Theses difficulties can be overcome by the mapping method. The experimental mapping method validated the efficiency calculation by comparison with the efficiencies of the cylindrical and Marinelli geometry CRM. The mapping of measured efficiency to calculated efficiency was consistent within 3 % of the uncertainty range. The validity of the simulation was done by checking the energy and position dependencies. Efficiency ratios were measured and simulated across three areas. As we verify the efficiency ratio, we confirm that the extended geometry can be dealt with through measurements and Monte Carlo simulations [20-23]. Therefore, it was confirmed that precise measurement of volume samples was possible when measured at each point around the detector.

References

[1] J. C. Hardy, V. E. Iacob, M. Sanchez-Vega, R. T. Effin-

ger, P. Lipnik, V. E. Mayes, D. K. Willis, and R. G. Helmer, Appl. Radiat. Isot. **56**, 65 (2002).
[2] O. Sima and D. Arnold, Appl. Radiat. Isot. **56**, 71 (2002).
[3] S. Kaminski, A. Jakobi, and Chr. Wilhelm, Appl. Radiat. Isot. **94**, 306 (2014).
[4] O. Alan, Nucl. Instr. and Meth. **274**, 297 (1989).
[5] V. V. Golovko, Appl. Radiat. Isot. 187 (2022).
[6] M. A. Ludington and R. G. Helmer, Appl. Radiat. Iso. **446**, 506 (2000).
[7] O. B. Ewa, D. Bodizs, and S. Czifrus, Appl. Radiat. Isot. **55**, 103 (2001).
[8] S. Nakamura, A. Wakita, et al., Appl. Radiat. Isot. **125**, 80 (2017).
[9] F. Salvat, J. M. Fernandez-Varea, and J. Sempau, France, 7-10 July. 2003.
[10] J. G. Guerra, J. G. Rubiano, G. Winter, M. A. Arnedo, et al. Nucl. Instr. and Meth. **908**, 206 (2018).
[11] GEANT: CERN Geneva, Switzerland.
[12] S. Hurtado, M. Garcia-Leon, and R. Garcia-Tenorio, Appl. Radiat. Isot. **61**, 139 (2004).
[13] G. S. C. Joel, N. M. Maurice, et al., Environ. Radio. **189**, 109 (2018).
[14] J. C. Hardy, V. E. Iacob, and M. Sanchez-Vega, Appl. Radiat. Isot. **56**, 65 (2002).
[15] N. Mezerreg, A. Azbouche, and M. Haddad, Environ. Radio. 232 (2021).
[16] A. Azbouche, M. Belgaid, and H. Mazrou, Environ. Radio. **146**, 119 (2015).
[17] A. Hamzawy, Nucl. Instr. and Meth. **624**, 125 (2010).
[18] A. Thabet and A. Hamzawy, Nucl. Eng. and Tech. **52**, 1271 (2020).
[19] S. Y. Park, et al., Appl. Radiat. Isot. 193 (2023).
[20] M. Omer, M. Koizumi, and R. Hajima, Radiat. Phys. Chem. 198 (2022).
[21] M. Lin, Y. Wang, and Z. Qin, Appl. Radiat. Isot. 200 (2023).
[22] E. Uyar and M. Bolikdemir, J. Instrum. 16 (2021).
[23] V. Lohrabian, A. Kamali-Asl, H. G. Harvani, S. R. Hosseini, and H. Zaidi, Radiat. Phys. Chem. 189 (2021).